Effective diffusivity and mass flux across the sediment-water interface in streams

Stanley B. Grant,[1,2] Michael J. Stewardson,[2] and Ivan Marusic[3]

Received 15 July 2011; revised 5 March 2012; accepted 5 March 2012; published 19 May 2012.

[1] The exchange of water between a stream and its hyporheic zone (defined as the sediment beneath and immediately adjacent to a stream) underpins many ecological and hydrological functions in turbulent streams. Hyporheic exchange can be parameterized in terms of an effective diffusion coefficient D_{eff} and considerable effort has gone into developing process-based models and empirical correlations for predicting the value of this transport parameter. In this paper we demonstrate previous laboratory estimates for D_{eff} can be biased by as much as a factor of 10, due to errors in the equations and/or ambiguities in the variables used to reduce data from transient tracer experiments in flow-through and recirculating flumes. After correcting these problems, an analysis of 93 previously published flume experiments reveals D_{eff} depends on properties of the tracer (molecular diffusivity), flow field (shear velocity, kinematic viscosity), and sediment bed (permeability and depth). The shear velocity depends implicitly on the Darcy-Weisbach friction factor, which captures the influence of bed roughness and bed forms on hyporheic exchange in both laboratory and field studies. The dependence of D_{eff} on sediment bed depth is consistent with the hypothesis that coherent turbulence in the water column drives mass transport across the sediment-water interface. Furthermore, the dependence of D_{eff} on sediment bed depth raises the possibility that hyporheic exchange rates measured in the laboratory are not representative of hyporheic exchange rates in the field.

Citation: Grant, S. B., M. J. Stewardson, and I. Marusic (2012), Effective diffusivity and mass flux across the sediment-water interface in streams, *Water Resour. Res.*, *48*, W05548, doi:10.1029/2011WR011148.

1. Introduction

[2] Stream health and function are inextricably linked to the hyporheic zone, defined as the region directly beneath and adjacent to a stream which contains some proportion of channel water [*Boulton et al.*, 2010; *Bencala et al.*, 2011]. Steep biogeochemical gradients in the hyporheic zone support a unique community of benthic and interstitial microorganisms [*Brunke and Gonser*, 1997] that cycle carbon, energy, and nutrients [*Malard et al.*, 2002; *Pinay et al.*, 2009; *Hinkle et al.*, 2001], and decontaminate the overlying water column [*Gandy et al.*, 2007]. The hyporheic zone also regulates stream temperature and sediment budgets, and serves as a spawning ground for fish [*Greig et al.*, 2007], refuge for benthic organisms [*Dole-Olivier et al.*, 1997; *Wood et al.*, 2010], and a rooting zone for aquatic plants [*Buss et al.*, 2009]. All of these functions require vigorous exchange of mass, heat, and momentum across the sediment-water interface, which can be compromised by a wide range of human activities, from channel and floodplain modifications to the conversion of drainage areas to urban and agricultural uses [*Brunke and Gonser*, 1997; *Hancock*, 2002]. For these and other reasons, stream restoration efforts increasingly include features—such as the introduction of pools, riffles, steps, debris dams, bars, meander bends, and side channels—that promote the exchange of water, mass, and heat between the stream and its hyporheic zone [*Hester and Gooseff*, 2010; *Boulton*, 2007; *Boulton et al.*, 2010; *Kasahara et al.*, 2009]. Such efforts would benefit from the ability to predict local transport rates across the sediment-water interface based on readily measureable properties of a stream.

[3] In general, hyporheic exchange occurs over a hierarchy of spatial scales, from single grains to entire catchments [*Buss et al.*, 2009; *Tonina and Buffington*, 2007; *Stonedahl et al.*, 2010; *Bencala et al.*, 2011]. At the local or "patch" scale (approximately 1 to 10 m), hyporheic exchange is likely determined by a number of phenomena, including (1) time averaged pressure gradients associated with geomorphic features such as riffles and pools [*Tonina and Buffington*, 2007] and the detachment and reattachment of the turbulent boundary layer over roughness elements on the sediment bed such as ripples, dunes, and cobbles [*Elliot and Brooks*, 1997a, 1997b; *Reidenbach et al.*, 2010]; (2) entrapment and release of pore water as a result of mobilization and deposition of boundary sediments caused by, for

[1]Department of Civil and Environmental Engineering and Department of Chemical Engineering and Materials Science, Henry Samueli School of Engineering, University of California, Irvine, California, USA.
[2]Department of Infrastructure Engineering, Melbourne School of Engineering, University of Melbourne, Victoria, Australia.
[3]Department of Mechanical Engineering, Melbourne School of Engineering, University of Melbourne, Victoria, Australia.

0043-1397/12/2011WR011148

example, the downstream migration of dunes and ripples [*Elliot and Brooks*, 1997a; *Elliot*, 1991]; (3) fluctuations in the pressure distribution caused by eddying motions in the stream that operate over a large range of spatial and temporal scales [*Fries*, 2007; *Packman et al.*, 2004; *Higashino et al.*, 2009; *Boano et al.*, 2011]; and (4) variations in sediment permeability that affect the rate at which water moves in and out of the sediment bed in response to both steady and fluctuating pressure distributions [*Buss et al.*, 2009; *Worman et al.*, 2002]. These interfacial transport processes and site-specific geomorphic and geological features drive hyporheic exchange across the sediment-water interface and can be parameterized with an effective diffusion coefficient D_{eff}. Several process-based models have been proposed for the effective diffusion coefficient [*Elliot and Brooks*, 1997a; *Packman et al.*, 2004; *Higashino et al.*, 2009] and recently *O'Connor and Harvey* [2008] (hereafter referred to as OH2008) developed an empirical correlation for D_{eff} based on a meta-analysis of previously published hyporheic exchange studies:

$$D_{\text{eff}}/D'_m = 5 \times 10^{-4} Re_k Pe_K^{6/5}. \tag{1}$$

[4] The Reynolds roughness number $Re_k = k_s u_* / \upsilon$ represents the height of roughness elements on the sediment bed k_s normalized by the "inner region" length scale for the viscous sublayer υ/u_*, where υ is the kinematic viscosity of water and the shear velocity u_* is a measure of bed shear stress [*Grant and Marusic*, 2011]. The roughness height k_s depends, in turn, on the characteristic grain diameter d_{90} (the 90th percentile of the grain size distribution), and the wavelength (λ) and amplitude (Δ) of bedforms (e.g., ripples and dunes) present at the sediment-water interface [*van Rijn*, 1984]:

$$k_s = 3d_{90} + 1.1\Delta(1 - e^{-25\Delta/\lambda}). \tag{2}$$

[5] The Peclet number $Pe_K = u_* \sqrt{K}/D'_m$ is a nondimensional grouping of the shear velocity (u_*), sediment permeability (K), and a molecular diffusion coefficient for tracer in sediment (D'_m) that depends on the molecular diffusion coefficient of the tracer in water (D_m) and the tortuosity of the pore network estimated from the sediment bed's porosity (θ) [*Iversen and Jorgensen*, 1993]:

$$D'_m = \frac{D_m}{1 + 3(1 + \theta)}. \tag{3}$$

[6] In this paper we revisit OH2008's empirical correlation for D_{eff} (equation (1)), focusing specifically on the fundamental formulas these researchers used to estimate values of D_{eff} from previously published laboratory studies of hyporheic exchange. The paper is organized as follows. We begin by presenting the mass transfer theory that underpins the use of effective diffusivity to parameterize hyporheic exchange, and correct errors in the formulas used by OH2008 and others to estimate D_{eff} from tracer measurements in recirculating and flow-through flumes (section 2). Multiple linear regression is then used to derive two new empirical correlations for D_{eff}, one based on primary variables and a second based on nondimensional groupings of primary variables (section 3). The paper concludes with a discussion of how new empirical correlations for D_{eff} inform current debate over the proper parameterization of bed roughness and bed forms, the extent to which hyporheic exchange measurements in the laboratory can be applied to the field, and the importance of coherent turbulence in the water column as a driving force for hyporheic exchange (section 4).

2. Parameterization of Hyporheic Exchange With Effective Diffusivity

[7] The use of effective diffusivity to parameterize hyporheic exchange is premised on the idea that mass transport in the sediment bed can be modeled by Fick's second law for the unsteady one-dimensional diffusion of mass in a homogeneous porous medium [*Incropera et al.*, 2007]:

$$\frac{\partial}{\partial t}(\theta C_s) = \frac{\partial}{\partial y}\left(\theta D_{\text{eff}} \frac{\partial C_s}{\partial y}\right). \tag{4}$$

[8] Variables appearing in equation (4) are defined in Figure 1. Assuming an infinitely deep sediment bed (i.e., $d_b \to \infty$ in Figure 1), a fixed tracer concentration at the sediment-water interface [$C_s(0,t) = C_{w,0}$], constant porosity θ, and an initial tracer concentration in the sediment pore fluids of $C_s(y,0) = C_{s,0}$, equation (4) can be solved exactly [*Incropera et al.*, 2007]:

$$\frac{C_s(y,t) - C_{w,0}}{C_s, 0 - C_{w,0}} = \text{erf}\left(\frac{y}{\sqrt{4D_{\text{eff}}t}}\right). \tag{5}$$

[9] An exact solution of equation (4) also exists for a sediment bed of finite thickness [*Incropera et al.*, 2007], although the "semi-infinite sediment bed" solution (equation (5)) is sufficient for the purposes of this study. The flux of tracer across the sediment side of the sediment-water interface can be derived from equation (5):

$$J_y^{\text{sediment}} = -D_{\text{eff}} \frac{\partial C_s}{\partial y}\bigg|_{y=0} = (C_{w,0} - C_{s,0}) \sqrt{\frac{D_{\text{eff}}}{\pi t}}. \tag{6}$$

[10] OH2008's meta-analysis included several different experimental approaches for estimating D_{eff}. Broadly speaking, all of these experimental approaches involve establishing an initial disequilibrium between the concentration of tracer in the water column and sediment (i.e., $C_{w,0} \neq C_{s,0}$), and then measuring the system's response as it comes to a new equilibrium. These different approaches can be broadly grouped into one of two types (referred to here as "Type I" or "Type II") depending on the nature of the initial condition (tracer added to the water column or to the sediment bed) and flume configuration (recirculating or flow-through, see Figure 1). In the sections 2.1, 2.2, and 2.3 we describe the different experimental approaches for estimating D_{eff} and correct historical errors in the formulas used to reduce primary data where appropriate. Key attributes of each experimental approach are listed in Table 1, including: (1) time series measurements from which the effective diffusivity is calculated; (2) the approach (e.g., formula) used to calculate a numerical estimate for D_{eff}; (3) the number of

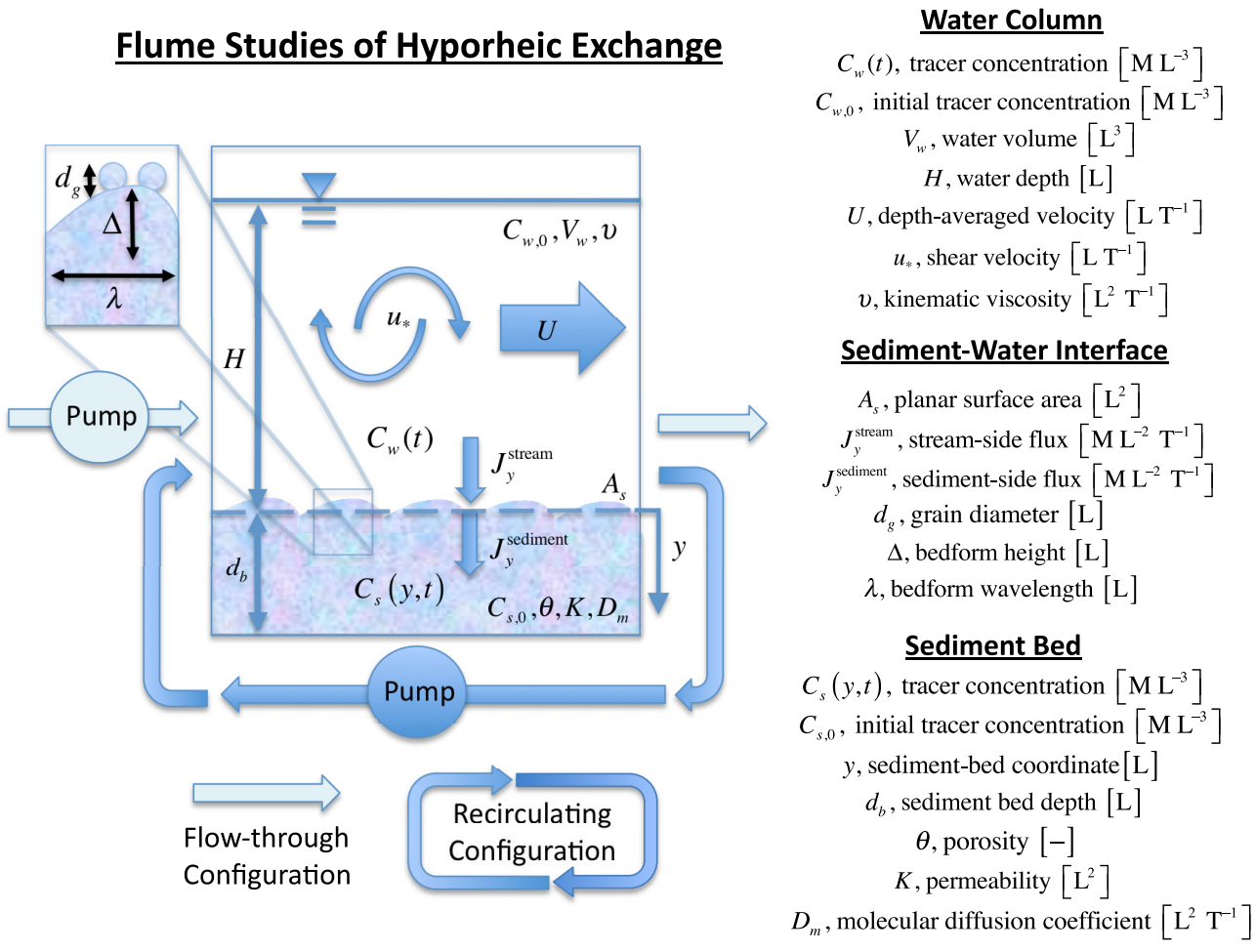

Figure 1. A schematic illustration of flow-through and recirculating flume experiments from which estimates of the effective diffusion coefficient are obtained.

Table 1. Summary of Formulas Used to Estimate the Effective Diffusion Coefficient for Hyporheic Exchange From Recirculating and Flow-Through Laboratory Flume Studies

Study Type	Formula[a] Corrected	Formula[a] OH2008	N[b]	Studies Using This Approach
Type I. Tracer Addition to the Water Column of Recirculating Flume ($C_{w,0} > 0$, $C_{s,0} = 0$)				
Type I.A Based on time series measurements of: $C^*(t) = C_w(t)/C_{w,0}$	$D_{\mathrm{eff}} = \frac{\pi}{4}\left(\frac{V_w}{A_s\theta}S\right)^2$, $S \equiv dC^*/d\sqrt{t}$	$D_{\mathrm{eff}} = \frac{\pi}{4}\left(\frac{V_w}{A_s}S\right)^2$	31 (33%)	*Rehg et al.* [2005]; *Packman et al.* [2004]; *Ren and Packman* [2004]; *Packman and MacKay* [2003]; *Marion et al.* [2002]; *Packman et al.* [2000b]
Type I.B Based on time series measurements of: $\ell(t) = \frac{V_w}{A_s\theta}[1 - C^*(t)]$	$D_{\mathrm{eff}} = \frac{\pi}{4}S_\ell^2$, $S_\ell \equiv d\ell/d\sqrt{t}$		20 (22%)	*Elliot and Brooks* [1997b]; *Tonina and Buffington* [2009]
Type I.C Based on time series measurements at fixed depth y ("breakthrough curves") of: $C_s(y,t)$	D_{eff} obtained by fitting analytical solution of equation (4) to breakthrough curves		9 (10%)	*Nagaoka and Ohgaki* [1990]
Type II. Tracer Addition to the Sediment Column of a Flow-Through Flume ($C_{w,0} = 0$, $C_{s,0} > 0$)				
Type II.A Based on time series measurements of: $M_w''(t) = \frac{UHW}{A_s}\int_0^t C_w(t)dt$	$D_{\mathrm{eff}} = \frac{\pi}{4}\left(\frac{S_{M_w}}{\theta C_{s,0}}\right)^2$, $S_{M_w} \equiv dM_w''/d\sqrt{t}$	$D_{\mathrm{eff}} = \frac{\pi}{4}\left(\frac{S_{M_w}}{C_{s,0}}\right)^2$	33 (35%)	*Richardson and Parr* [1988]; *Lai et al.* [1994]

[a]OH2008s original formula is provided in cases where it has been has been corrected in this paper.
[b]Number of D_{eff} values calculated by this approach included in OH2008s meta-analysis.

D_{eff} values calculated by this approach in OH2008's meta-analysis; and (4) studies from which the primary data were obtained.

2.1. Tracer Addition to the Water Column of a Recirculating Flume (Type I)

[11] Recirculating flumes are configured so water exiting the downstream end of the flume is pumped through pipes back to the upstream end of the flume. In this configuration, a finite volume of water continuously circulates through the flume in a closed loop (Figure 1). In a typical recirculating flume experiment, a nonreactive tracer is added to the water column of an initially tracer-free flume. The initial condition is therefore a nonzero concentration of tracer in the water column ($C_{w,0} > 0$) and a null concentration of tracer in the sediment bed ($C_{s,0} = 0$). Ambient turbulence quickly mixes the tracer over the water column, and the tracer slowly penetrates into the interstices (pore fluids) of the sediment bed. As tracer penetrates into the sediment bed, the well-mixed concentration of tracer in the water column [$C_w(t)$] declines, while the concentration of tracer in sediment interstices [$C_s(y,t)$] increases. To minimize initial oscillations of $C_w(t)$, tracer is typically metered into the water column over the residence time of the water in the flume, $\tau = V_w/Q$, where V_w represents the volume of water in the flume (including all water overlying the sediment bed and water in the plumbing used to recirculate the water, but excluding pore water in the sediment bed) and Q is the volumetric flow rate of the recirculated water [e.g., see discussion of methods by *Rehg et al.*, 2005]. For Type I experiments, three experimental approaches have been adopted for estimating D_{eff}, based on the quantity measured over the course of the experiment, as described next.

2.1.1. Recirculating Flume: Measurements of Tracer Concentration in the Water Column (Type I.A)

[12] In this approach, measurements of tracer concentration in the water column are converted directly into estimates of effective diffusivity. This is accomplished by invoking tracer mass balance in the water column (equation (9) in OH2008's paper):

$$J_y^{\text{stream}} = -\frac{V_w}{A_s}\frac{dC_w}{dt}. \tag{7}$$

[13] The variable J_y^{stream} represents the flux of tracer into the sediment bed as observed from the stream side of the sediment-water interface (see Figure 1). A subtle but important issue now arises, regarding the correct matching condition for the flux of tracer across the stream side (J_y^{stream}, equation (7)) and sediment side (J_y^{sediment}, equation (6)) of the sediment-water interface. OH2008 assumes $J_y^{\text{stream}} = J_y^{\text{sediment}}$, which yields the following expression for tracer concentration in the water column (equation (10) in their paper):

$$C^*(t) = 1 - \frac{2A_s}{V_w}\left(\frac{D_{\text{eff}}t}{\pi}\right)^{1/2}. \tag{8}$$

[14] The variable $C^*(t) = C_w(t)/C_{w,0}$ is the normalized concentration of tracer in the water column. According to equation (8), a plot of $C^*(t)$ against $\sqrt{t}$ should yield a slope $S = dC^*/d\sqrt{t} = -2A_s\sqrt{D_{\text{eff}}/\pi}/V_w$. From a rearrangement of the last expression, the effective diffusion coefficient can be estimated directly from experimental measurements of the slope S and flume geometry (A_s, V_w) (equation (11) in OH2008):

$$D_{\text{eff}} = \pi\left(\frac{V_w}{2A_s}S\right)^2. \tag{9}$$

[15] However, by equating J_y^{stream} and J_y^{sediment}, OH2008 assumes transport of the tracer occurs across the same surface area on both sides of the sediment-water interface when, in fact, the tracer can only penetrate into void spaces on the sediment side of the interface (see Figure 1). The correct matching condition should therefore be $J_y^{\text{stream}} = \theta J_y^{\text{sediment}}$ which yields new expressions for the normalized concentration and effective diffusion coefficient:

$$C^*(t) = 1 - \frac{2A_s\theta}{V_w}\left(\frac{D_{\text{eff}}t}{\pi}\right)^{1/2}, \tag{10a}$$

$$D_{\text{eff}} = \pi\left(\frac{V_w}{2A_s\theta}S\right)^2. \tag{10b}$$

[16] Equations (9) and (10b) differ by a factor of $1/\theta^2$ which, for a typical bed porosity of around $\theta = 0.3$, implies OH2008's formula for D_{eff} (equation (9)) underestimates the effective diffusion coefficient by about an order of magnitude.

2.1.2. Recirculating Flume: Measurements of Effective Depth of Solute Penetration (Type I.B)

[17] The transfer of tracer into the sediment bed of a recirculating flume can also be represented by a length-scale ℓ called the "effective depth of solute penetration." The effective depth of solute penetration represents the depth in the sediment bed to which the tracer would theoretically extend if it were mixed down to that depth at the initial concentration of the tracer in the water column $C_{w,0}$. Given this definition, a mass balance of the tracer within the flume yields the following relationship between the effective depth of penetration and the normalized concentration of tracer in the overlying water column:

$$\ell(t) = \frac{V_w}{A_s\theta}[1 - C^*(t)]. \tag{11}$$

[18] Given this definition, and assuming porosity does not change with depth or time, the total mass of tracer in the sediment bed $m_s(t)$ at any time t can be expressed in terms of either $\ell(t)$ (equation (12a)) or $C_s(y,t)$ (equation (12b)):

$$m_s(t) = C_{w,0}\ell(t)A_s\theta, \tag{12a}$$

$$m_s(t) = \theta A_s\int_0^\infty C_s(y,t)dy. \tag{12b}$$

[19] Equating these two expressions and substituting the solution for $C_s(y,t)$ (equation (5)) yields the following relation between $\ell(t)$ and the effective diffusion coefficient D_{eff}:

$$\ell(t) = 2\left(\frac{D_{\text{eff}}t}{\pi}\right)^{1/2}. \tag{13}$$

[20] Based on equation (13), the effective diffusion coefficient can be estimated from experimental measurements of the slope $S_\ell \equiv d\ell/d\sqrt{t}$ (equation (20) in OH2008):

$$D_{\text{eff}} = \frac{\pi}{4}S_\ell^2. \tag{14}$$

[21] The length-scale ℓ has taken on different notation in the literature, including "M'/θ" by OH2008, "$m(t)/\theta$" by *Elliot* [1991] and *Elliot and Brooks* [1997b], and "$m_e(t)$" by *Tonina and Buffington* [2007].

[22] There is another definition of the effective penetration depth that, when used in conjunction with equation (14), can result in a small but systematic error in the estimated value of D_{eff}. *Elliot* [1991] and *Elliot and Brooks* [1997b] define a length-scale ℓ' that represents the depth to which tracer would theoretically extend into the sediment bed if it were mixed down to that depth at the instantaneous concentration in the overlying water column, $C_w(t)$:

$$\ell'(t) = \frac{\ell(t)}{C^*(t)} = \frac{V_w}{A_s\theta}\left[\frac{1}{C^*(t)} - 1\right]. \tag{15}$$

[23] For this choice of length scale, the accumulation of tracer mass in the sediment bed is given by

$$m_s(t) = \mathrm{C}_w(t)\ell'(t)A_s\theta. \tag{16}$$

[24] Equating equations (16) and (12b) yields, after substituting equations (5) and (15), the following relationship between ℓ' and D_{eff}:

$$\ell' = \frac{2}{C^*(t)}\sqrt{\frac{D_{\text{eff}}}{\pi}}. \tag{17}$$

[25] Comparing equations (13) and (17), it is clear that $\ell' \geq \ell$, which implies substitution of ℓ' for ℓ in equation (14) will yield estimates for the effective diffusivity that are larger than the true value. A number of notational permutations have been adopted for ℓ' in the literature, including "m" [*Packman et al.*, 2004; *Rehg et al.*, 2005; *Packman and MacKay*, 2003], "M" [*Packman et al.*, 2000b], "M/θ" [*Elliot and Brooks*, 1997a, 1997b; *Elliot*, 1991], and "M_e" [*Tonina and Buffington*, 2007].

[26] Given the potential confusion caused by having an alternative definition of the effective penetration depth, one might wonder why ℓ' was adopted as a measure of hyporheic exchange (e.g., see *Elliot* [1991]). Probable explanations include: (1) The quantity ℓ' is conceptually easy to understand and has elegant physical limits: $\ell' = 0$ at $t = 0$ to $\ell' = d_b$ at $t \to \infty$, where d_b is the depth of the sediment bed (see equation (15)). By contrast, the interpretation of ℓ is less obvious, and its physical limits less intuitive: $\ell = 0$ at $t = 0$ to $\ell = d_b(1 + d_b\theta A_s/V_w)^{-1}$ at $t \to \infty$ (see equation (11)). The equations given here for ℓ and ℓ' in the limits of a long time ($t \to \infty$) correspond to a final (or equilibrium) condition, when the normalized concentration of the tracer in the water column and sediment pores equal $C_f^* = C_f/C_{w,0} = (1 + A_s\theta d_b/V_w)^{-1}$. (2) The formulas for estimating D_{eff} from ℓ' and ℓ are identical in the event tracer concentration and the water column is constant over the period of analysis, $C_w(t) = C_{w,0}$. The approximation $C_w(t) \approx C_{w,0}$ was already invoked to obtain a solution for $C_s(y,t)$ [i.e., the upper boundary condition for that solution is $C_s(y = 0, t) = C_{w,0}$, see equation (5)], and so it could be argued little harm comes from invoking it again, although in the first instance the rate of mass transfer into the sediments is overestimated, while in the second instance tracer mass balance over the flume is violated. The proliferation of different notation in the literature for both ℓ' and ℓ can make understanding what length scale is being reported difficult.

2.1.3. Recirculating Flume: Measurements of Tracer Breakthrough in the Sediment Bed (Type I.C)

[27] *Nagaoka and Ohgaki* [1990] estimated the effective diffusion coefficient for hyporheic exchange by measuring in situ breakthrough curves of a conservative tracer (NaCl) in the sediment column of a recirculating flume. Experiments were conducted by adding tracer to the water column of an initially tracer-free flume, and thus the initial conditions were a nonzero concentration of tracer in the water column ($C_{w,0} > 0$) and a null concentration of tracer in the sediment bed ($C_{s,0} = 0$). From conductivity probes placed at various depths in the sediment column, time series measurements of NaCl concentration (or "breakthrough curves") were obtained, and numerically fit to an analytical solution of the one-dimensional diffusion equation (equation (4)) to obtain experimental estimates for D_{eff}. The values of D_{eff} obtained by this approach decrease with depth into the bed. For their meta-analysis, OH2008 adopted the values of D_{eff} measured closest to the sediment-water interface.

2.2. Tracer Addition to the Sediment Bed of a Flow-Through Flume (Type II)

[28] Flow-through flume experiments are configured so water makes a single pass through the flume. In a typical flow-through flume experiment, tracer-free water is flowed over the top of a sediment bed containing a conservative tracer in the pore fluids. The initial condition is therefore a zero concentration of tracer in the water column ($C_{w,0} = 0$) and a nonzero concentration of tracer in the sediment bed ($C_{s,0} > 0$). The total mass of tracer released from the sediment bed at any elapsed time t can be estimated from time series measurements of the tracer concentration in the water discharged from the downstream end of the flume [$C_w(t)$]:

$$M_w(t) = \int_0^t C_w(t)UHWdt. \tag{18}$$

[29] In this last equation, U, H, W are the flow velocity, water depth, and width of the flume, respectively. For a conservative tracer, the total mass exiting the flume must equal the total mass released from the sediment bed:

$$M_w(t) = -A_s\theta\int_0^t J_y^{\text{sediment}}dt = 2\theta A_s C_{s,0}\sqrt{\frac{D_{\text{eff}}t}{\pi}}. \tag{19}$$

[30] Based on equation (19), the effective diffusion coefficient can be estimated from the slope $S_{M_w} \equiv dM_w''/d\sqrt{t}$, where $M_w'' = M_w/A_s$:

$$D_{\text{eff}} = \pi \left[\frac{S_{m_w}}{2\theta C_{s,0}} \right]^2. \quad (20)$$

[31] In OH2008, values of D_{eff} were obtained from a form of equation (20) that does not include a porosity term (equation (28) in OH2008):

$$D_{\text{eff}} = \pi \left[\frac{S_{m_w}}{2C_{s,0}} \right]^2. \quad (21)$$

[32] This error appears to have originated from several early papers [*Richardson and Parr*, 1988; *Parr et al.*, 1987] in which the solution for unsteady loss of heat from a semi-infinite solid by conduction and convection was adopted without accounting for sediment porosity; i.e., the flux boundary condition at the sediment-water interface, as expressed by equation (5) by *Parr et al.* [1987] and equation (10) by *Richardson and Parr* [1988], should have accounted for the fact that tracer can only "diffuse" through void spaces in the sediment. Thus, in OH2008's meta-analysis, estimates of the effective diffusion coefficient obtained from flow-through tracer experiments reported previously by *Richardson and Parr* [1988] and *Lai et al.* [1994] are biased low by $\theta^{-2} \approx 10$.

2.3. Summary of Methods for Estimating the Effective Diffusion Coefficient

[33] The majority (64 out of 93, or 69%) of D_{eff} values in OH2008's meta-analysis were estimated using Type I.A and Type II approaches; importantly, both approaches employed formulas that underestimate the true D_{eff} by about one order of magnitude. The other 29 D_{eff} values were estimated using approaches that either overestimate the true value [Type I.B if $\ell'(t)$ is substituted into equation (13)] or have no known bias [Type I.C and Type I.B if $\ell(t)$ is substituted into equation (13)]. Because all 93 D_{eff} values were included in OH2008's regression analysis, the varying sign and magnitude of bias (ranging from none to more than a factor of 10) must have impacted the empirical correlation for D_{eff} proposed by OH2008 (equation (1) in this paper).

3. New Correlation for D_{eff}

3.1. Overview

[34] In sections 3.1 through 3.3 we assess whether correction of the errors and issues raised above, and improvements in the statistical methods used to carry out the regression step, substantially alter OH2008's empirical correlation for D_{eff} (equation (1)). Based on the list of variables indicated in Figure 1, the effective diffusion coefficient could depend on as many as nine independent variables (see Figure 1 for definitions):

$$D_{\text{eff}} = f(D_m, U, u_*, k_s, K, \upsilon, H, d_b, \theta). \quad (22)$$

[35] The variables $C^* = C_w(t)/C_{w,0}$, $C_s(y,t)$, J_y^{stream}, J_y^{sediment} appear in Figure 1, but are not included on the right-hand side of equation (22) because they are important only in so far as they are needed to estimate values of D_{eff} using the approaches summarized in Table 1 and described in section 2. In addition, grain diameter (d_{90}), bed form amplitude (Δ), and bed form wavelength (λ) are collapsed into the roughness length scale k_s (see equation (2)). The list of variables on the right-hand side of equation (22) includes several not considered in OH2008's correlation analysis, including water depth H, sediment bed depth d_b, and porosity θ (although porosity was included implicitly in OH2008's tortuosity modified form of the molecular diffusion coefficient D_m', see equation (3)). In sections 3.2 and 3.3 we employ multiple linear regression (MLR) to derive a new set of empirical correlations for D_{eff}.

3.2. Multiple Linear Regression: Methods

[36] MLR analysis was implemented with freeware (US EPA Virtual Beach 2.0, http://www.epa.gov/ceampubl/swater/vb2/) [*Frick et al.*, 2008; *Ge and Frick*, 2007] subject to the following conditions. Independent variables were excluded from the regression if their variance inflation factor (VIF) exceeded 5, indicating significant correlation with other independent variables, or "multicollinearity." Retaining independent variables that exhibit significant multicollinearity can adversely affect the matrix inversion step required to obtain predictor variable coefficients, and cause the predicted coefficients to change erratically in response to small changes in the data upon which the regression is carried out [*Longnecker and Ott*, 2004]. An exhaustive set of potential models was then created involving all possible combinations of nonexcluded independent variables, and each model was subsequently ranked according to their corrected Akaike information criterion (AIC) value, which accounts for the trade-off between model complexity and goodness of fit [*Akaike*, 1974]. In this scheme, the "best" models have a low corrected AIC value, indicating an optimal trade-off between predictive power and parsimony.

[37] The set of hyporheic exchange studies included in the MLR are summarized in Table 2. Also shown in the table are values of effective diffusivity as they appear in OH2008's meta-analysis ($D_{\text{eff}}^{\text{OH2008}}$), and after correcting errors identified in section 2 ($D_{\text{eff}}^{\text{This Study}}$). Effective diffusivities estimated from Type I.A and Type II.A studies were all corrected by dividing $D_{\text{eff}}^{\text{OH2008}}$ by θ^{-2}. *Elliot and Brooks* [1997b] reported values of $\ell'(t)$, which overestimate D_{eff} when substituted into equation (14) (section 2.4). To correct this error, we converted values of $\ell'(t)$ to $C^*(t)$ using a rearranged form of equation (15), and then estimated values of $D_{\text{eff}}^{\text{This Study}}$ from equation (10b). *Tonina and Buffington* [2007] also report their results in terms of $\ell'(t)$, but Tonina kindly provided the raw $C^*(t)$ data (personal communication) which we substituted into equation (10b) to estimate $D_{\text{eff}}^{\text{This Study}}$. Effective diffusivities estimated from Type I.C studies were unchanged; i.e., $D_{\text{eff}}^{\text{This Study}} = D_{\text{eff}}^{\text{OH2008}}$. O'Connor compiled values of the nine independent variables appearing on the right-hand side of equation (22) for all 93 hyporheic exchange experiments, and kindly provided the compiled data for this study (personal communication); values of the independent variables were checked against the primary studies from which they were derived, and a few transcriptional errors corrected (Table A1).

Table 2. Summary of Previously Published Flume Data Included in This Study[a]

Source, Tracer	Expt.	Bed Form	Experiment Type	$D_{\text{eff}}^{\text{OH2008}}$ ($m^2\ s^{-1}$)	$D_{\text{eff}}^{\text{This Study}}$ ($m^2\ s^{-1}$)
Richardson and Parr [1988], Fluorescein	a6	Plane	II.A	3.13E-09	2.17E-08
	d1	Plane	II.A	2.93E-09	1.83E-08
	d1r	Plane	II.A	8.69E-09	5.43E-08
	d2	Plane	II.A	3.36E-10	2.10E-09
	d3	Plane	II.A	6.29E-09	3.93E-08
	b1	Plane	II.A	6.94E-09	4.80E-08
	b2	Plane	II.A	2.62E-09	1.81E-08
	b2r	Plane	II.A	7.12E-09	4.93E-08
	b5	Plane	II.A	5.50E-10	3.81E-09
	b5r	Plane	II.A	2.20E-09	1.52E-08
	b6	Plane	II.A	1.77E-10	1.22E-09
	b7	Plane	II.A	3.69E-09	2.55E-08
	b8	Plane	II.A	4.66E-10	3.23E-09
	b8r	Plane	II.A	8.30E-10	5.75E-09
	e1	Plane	II.A	1.25E-10	9.13E-10
	e1r	Plane	II.A	6.09E-10	4.44E-09
	e2	Plane	II.A	4.63E-10	3.38E-09
	e2r	Plane	II.A	1.67E-09	1.22E-08
	e3	Plane	II.A	5.88E-11	4.30E-10
	e4	Plane	II.A	1.52E-09	1.11E-08
	c1	Plane	II.A	2.86E-10	2.21E-09
	c1r	Plane	II.A	3.31E-10	2.56E-09
	c2	Plane	II.A	6.75E-11	5.21E-10
	c2r	Plane	II.A	1.45E-10	1.12E-09
	c3	Plane	II.A	3.36E-11	2.59E-10
Elliot and Brooks [1997b], NaCl	8	Bed form	I.B	3.03E-07	2.20E-07
	9	Bed form	I.B	2.96E-07	1.95E-07
	10	Bed form	I.B	5.41E-08	3.29E-08
	12	Bed form	I.B	1.49E-07	1.08E-07
	14	Bed form	I.B	5.41E-08	3.93E-08
	15	Bed form	I.B	1.51E-07	1.03E-07
	16	Bed form	I.B	3.52E-07	2.50E-07
	17	Bed form	I.B	1.28E-08	1.05E-08
Packman et al. [2000b], LiCl	7	Bed form	I.A	1.63E-08	1.54E-07
	13	Bed form	I.A	1.35E-08	1.28E-07
	15	Bed form	I.A	1.41E-08	1.33E-07
Marion et al. [2002], NaCl	S1	Plane	I.A	1.68E-07	1.16E-06
	S2	Ripples	I.A	3.20E-07	2.21E-06
	S3	Dunes/Ripples	I.A	3.77E-07	2.61E-06
	S4	Dunes	I.A	5.87E-07	4.06E-06
	S5	Dunes	I.A	9.79E-07	6.78E-06
Packman and McCay [2003], NaCl	1	Dunes	I.A.	9.38E-08	6.49E-07
	2a	Dunes	I.A	3.61E-08	2.50E-07
	2b	Dunes	I.A	2.10E-08	2.49E-07
	3a	Dunes	I.A	1.81E-08	1.25E-07
	3b	Dunes	I.A	1.09E-08	1.30E-07
Rehg et al. [2005], NaCl	1	Natural bed	I.A	7.94E-09	6.12E-08
	2	Natural bed	I.A	2.55E-08	1.97E-07
Tonina and Buffington [2007], Fluorescein	1	Pool-riffle	I.B	1.48E-05	5.10E-05
	2	Pool-riffle	I.B	1.17E-05	3.64E-05
	3	Pool-riffle	I.B	1.09E-05	4.09E-05
	4	Pool-riffle	I.B	1.19E-05	4.61E-05
	5	Pool-riffle	I.B	3.30E-05	1.38E-04
	6	Pool-riffle	I.B	1.83E-05	6.62E-05
	7	Pool-riffle	I.B	2.06E-05	7.23E-05
	8	Pool-riffle	I.B	1.51E-05	5.30E-05
	9	Pool-riffle	I.B	9.75E-06	3.90E-05
	10	Pool-riffle	I.B	9.41E-06	3.69E-05
	11	Pool-riffle	I.B	7.21E-06	3.50E-05
	12	Pool-riffle	I.B	4.56E-06	2.18E-05
Nagaoka and Ohgaki [1990], NaCl	1	Plane	I.C	6.46E-04	6.46E-04
	2	Plane	I.C	4.33E-04	4.33E-04
	3	Plane	I.C	1.55E-04	1.55E-04
	4	Plane	I.C	1.26E-04	1.26E-04
	5	Plane	I.C	9.09E-05	9.09E-05
	6	Plane	I.C	6.58E-05	6.58E-05
	10	Plane	I.C	1.51E-04	1.51E-04
	11	Plane	I.C	7.62E-05	7.62E-05
	12	Plane	I.C	1.88E-05	1.88E-05

Table 2. (continued)

Source, Tracer	Expt.	Bed Form	Experiment Type	$D_{\text{eff}}^{\text{OH2008}}$ ($m^2\ s^{-1}$)	$D_{\text{eff}}^{\text{This Study}}$ ($m^2\ s^{-1}$)
Ren and Packman [2004], NaCl	2	Bed form	I.A	3.16E-09	2.44E-08
	3	Bed form	I.A	7.69E-09	5.94E-08
	4	Bed form	I.A	4.83E-09	3.72E-08
	5	Bed form	I.A	1.08E-08	8.30E-08
	6	Bed form	I.A	1.97E-08	1.52E-07
Lai et al. [1994], KCl	a6	Plane	II.A	8.57E-08	5.94E-07
	a8	Plane	II.A	3.09E-09	2.14E-08
	a9	Plane	II.A	8.16E-09	5.65E-08
	b1	Plane	II.A	2.47E-08	1.71E-07
	b4	Plane	II.A	6.44E-09	4.46E-08
	b7	Plane	II.A	3.17E-09	2.20E-08
	c4	Plane	II.A	1.32E-08	9.61E-08
	d4	Plane	II.A	3.53E-09	2.73E-08
Packman et al. [2004], NaCl	1	Plane	I.A	2.29E-05	1.58E-04
	2	Plane	I.A	1.53E-05	1.06E-04
	3	Plane	I.A	6.65E-06	4.60E-05
	4	Plane	I.A	1.02E-06	7.08E-06
	5	Plane	I.A	1.77E-05	1.22E-04
	6	Plane	I.A	2.96E-06	2.05E-05
	7	Bed form	I.A	2.65E-05	1.83E-04
	8	Bed form	I.A	7.00E-06	4.85E-05
	9	Bed form	I.A	3.95E-05	2.73E-04
	10	Bed form	I.A	2.65E-05	1.83E-04
	11	Bed form	I.A	7.00E-06	4.85E-05

[a]Effective diffusion coefficients were either reported by *O'Connor and Harvey* [2008] ($D_{\text{eff}}^{\text{OH2008}}$) or calculated using the set of formulas recommended in this study ($D_{\text{eff}}^{\text{This Study}}$).

3.3. Multiple Linear Regression: Results

3.3.1. Independent Variables Predictive of D_{eff}

[38] As a first step, we set out to determine which of the independent variables on the right-hand side of equation (22) predict the value of D_{eff}. To that end we assumed a power law form for the function f which, after log-transformation, takes on the following linear form:

$$\log D_{\text{eff}}^{\text{This Study}} = \log a + b\log D_m + c\log U + d\log u_* + e\log k_s + f\log K + g\log \upsilon + h\log H + i\log d_b + j\log \theta. \quad (23)$$

[39] Values for the unknown coefficients $\{a, \ldots, j\}$ were determined by MLR, adopting $\log D_{\text{eff}}^{\text{This Study}}$ as the dependent variable and all the log-transformed variables on the right-hand side of equation (23) as independent variables. The two top-ranked models obtained by MLR are summarized in Table 3. These two models, which were selected from 511 candidate models, exclude D_m and k_s terms, and therefore coefficient values and statistics for these two variables are not included in the table. The two top-ranked models differ by the inclusion of kinematic viscosity in model 2. Regression coefficients for the other variables $(U, u_*, K, H, d_b, \theta)$ are the same within error, suggesting their power law exponents are robust. The top-ranked model implies the following empirical correlation for the effective diffusion coefficient:

$$D_{\text{eff}}^{\text{This Study}} = 10^{7.2} U^{0.83\pm0.2} u_*^{1.4\pm0.2} K^{0.91\pm0.03} H^{0.40\pm0.1} \times d_b^{0.68\pm0.12} \theta^{1.5\pm0.6}. \quad (24)$$

[40] This model accounts for 98% of the variance in $\log D_{\text{eff}}^{\text{This Study}}$ (i.e., $R^2 = 0.98$, see Table 3 and Figure 2).

3.3.2. Nondimensional Groups Predictive of D_{eff}

[41] The empirical correlation developed in section 3.3.1 (equation (24)) is not dimensionally homogeneous; i.e., the collection of variables on the right-hand side of the equation do not have units of diffusivity. Under such circumstances, the multiplicative constant ($10^{7.2}$) must take on units ($L^{-3.1}T^{1.2}$). Alternatively, a dimensionally homogeneous correlation can be created by conducting MLR with nondimensional groupings of the primary variables. Assuming 10 possible primary variables (see equation (22)) and two physical dimensions (length and time), the Buckingham Pi Theorem predicts that laboratory measurements of hyporheic exchange can be modeled with at most eight nondimensional groups [*Fischer et al.*, 1979]. While the Buckingham Pi Theorem predicts the maximum number of nondimensional groups required, the choice of these groups is, at this stage, largely an educated guess. As a starting point we assume effective

Table 3. MLR Output for the Two Top AIC Ranked Models (Out of 511 Candidate Models) Based on Equation (23)[a]

Independent Variable	Regression Coefficients		p Values	
	Model 1	Model 2	Model 1	Model 2
Intercept	$10^{7.2\pm0.47}$	$10^{3.2\pm4.3}$	2.9×10^{-26}	0.46
U	0.827 ± 0.182	0.806 ± 0.184	1.8×10^{-5}	3.2×10^{-5}
u_*	1.40 ± 0.156	1.41 ± 0.157	5.9×10^{-14}	5.4×10^{-14}
K	0.909 ± 0.033	0.905 ± 0.033	4.2×10^{-44}	2.8×10^{-43}
H	0.402 ± 0.096	0.397 ± 0.097	7.3×10^{-5}	8.9×10^{-5}
d_b	0.683 ± 0.121	0.682 ± 0.121	2.1×10^{-7}	2.4×10^{-7}
θ	1.49 ± 0.56	1.56 ± 0.57	0.0098	0.0075
υ	–	-0.664 ± 0.71	–	0.355

[a]The adjusted R^2 and corrected AIC values are 0.98 and −136 for the top-ranked model (model 1) and 0.98 and −134 for the second top-ranked model (model 2).

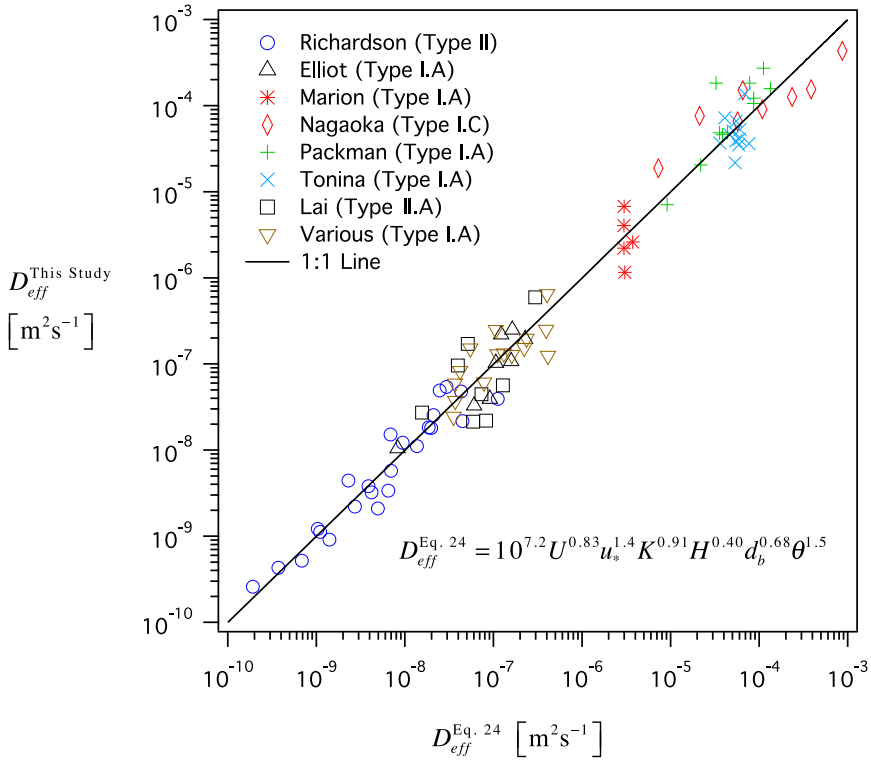

Figure 2. Comparison of measured effective diffusivities with those obtained from equation (24).

diffusivity can be expressed in nondimensional form as follows:

$$\frac{D_{\text{eff}}^{\text{This Study}}}{D_m} = F\left(Re = \frac{UH}{\upsilon}, Re_k = \frac{u_* k_s}{\upsilon}, Re_* = \frac{u_* H}{\upsilon}, Pe_* = \frac{u_* \sqrt{K}}{\upsilon}, Sc = \frac{\upsilon}{D_m}, \theta, \frac{u_* d_b}{\upsilon}\right). \tag{25}$$

[42] The set of nondimensional groups on the right-hand side of equation (25) were chosen because they collectively characterize stream hydrodynamics and boundary layer turbulence (Re, Re_k, Re_*) [*Sturm*, 2010; *Grant and Marusic*, 2011], interfacial mass transport (Schmidt number, Sc) [*Incropera et al.*, 2007], transport across the sediment-water interface (Pe_*, θ) [*Richardson and Parr*, 1988; *O'Connor and Harvey*, 2008], and flume-specific features of hyporheic exchange experiments ($u_* d_b/\upsilon$). In selecting this particular set of nondimensional groups, we introduced two primary variables (kinematic viscosity and the molecular diffusion coefficient) that are not strongly correlated with effective diffusivity (see MLR results, section 3.3.1). Inclusion of these two variables is justified, however, because they provide natural scales for the diffusion of momentum (υ) and mass (D_m) with which other variables (or collection of variables) can be normalized. Values for the set of nondimensional numbers appearing on the right-hand side of equation (25) are tabulated for all 93 hyporheic exchange experiments in the Appendix (Table A2).

[43] To determine which of the dimensionless groups on the right-hand side of equation (25) predict the value of $D_{\text{eff}}^{\text{This Study}}/D_m$, we carried out MLR as follows. We assumed a power law function for F which, after log-transformation, takes on the following linear form:

$$\log \frac{D_{\text{eff}}^{\text{This Study}}}{D_m} = \log a + b\log Re + c\log Re_k + d\log Re_* + e\log Pe_* + f\log Sc + g\log\theta + h\log\frac{u_* d_b}{\upsilon}. \tag{26}$$

[44] Values for the unknown coefficients $\{a, \ldots, h\}$ were determined by MLR, adopting $\log(D_{\text{eff}}^{\text{This Study}}/D_m)$ as the dependent variable, and the log-transformed nondimensional groups on the right-hand side of equation (26) as independent variables. The two top-ranked models obtained by MLR are summarized in Table 4. These two models, which were selected from 127 candidate models, exclude Re, Re_k, Re_* (model 1) or Re, Re_k, Re_*, Sc (model 2). Regression coefficients for the three nondimensional groups common to the two top-ranked models ($Pe_*, u_* d_b/\upsilon, \theta$) are the same within error (Table 4), suggesting their power law exponents are robust. The p value for the Schmidt number Sc in the top-ranked model is larger than the significance threshold of $p < 0.05$. Furthermore, the top two models are similar relative to their adjusted R^2 (0.972 versus 0.971) and corrected AIC (-133 versus -132). For all of these reasons, the more parsimonious model (i.e., model 2) was adopted (Figure 3):

$$\frac{D_{\text{eff}}^{\text{This Study}}}{D_m} = 240\left(\frac{u_*\sqrt{K}}{\upsilon}\right)^{1.6\pm0.07}\left(\frac{u_* d_b}{\upsilon}\right)^{0.7\pm0.08}\theta^{2.2\pm0.6}. \tag{27}$$

Table 4. MLR Output for the Two Top AIC Ranked Models (Out of 127 Candidate Models) Based on Equation (26)[a]

Independent Variable	Regression Coefficients		p Values	
	Model 1	Model 2	Model 1	Model 2
Intercept	$10^{1.63\pm0.54}$	$10^{2.38\pm0.37}$	0.0036	7.4×10^{-9}
$\log Pe_*$	1.64 ± 0.065	1.63 ± 0.065	6.6×10^{-42}	1.3×10^{-41}
$\log Sc$	0.23 ± 0.12	–	0.063	–
θ	2.19 ± 0.57	2.22 ± 0.58	0.0002	0.0002
$\log \frac{u_* d_b}{\upsilon}$	0.708 ± 0.075	0.692 ± 0.075	4.7×10^{-15}	1.7×10^{-14}

[a]The adjusted R^2 and corrected AIC values are 0.972 and −133 for the top-ranked model (model 1) and 0.971 and −132 for the second top-ranked model (model 2).

[45] The range of nondimensional groups over which this equation applies is as follows:

$$0.6 \leq \frac{D_{\text{eff}}^{\text{This Study}}}{D_m} \leq 4 \times 10^5,$$

$$0.01 \leq \frac{u_* \sqrt{K}}{\upsilon} \leq 20,$$

$$50 \leq \frac{u_* d_b}{\upsilon} \leq 1 \times 10^4,$$

$$0.2 \leq \theta \leq 0.4.$$

[46] Comparing the primary variable correlation (equation (24)) with the nondimensional group correlation (equation (27)), we find the former includes two variables not included in the latter (U, H), while the latter includes two variables not included in the former (υ, D_m). The variables U and H would logically appear in the form of the Reynolds number ($Re = UH/\upsilon$). Indeed, the Reynolds number does appear in four of the top ten models generated by MLR (just not in the top two included in Table 4), but only when the nondimensional bed depth number ($u_* d_b/\upsilon$) is excluded. The mutually exclusive nature of these two numbers is due to the fact that they are highly correlated [Pearson $R = 0.87$ for $\log Re$ versus $\log(u_* d_b/\upsilon)$] and therefore if one appears in a regression, the other has an elevated VIF (see MLR methods). The appearance of D_m and υ in equation (27) is an artifact of our decision to include these two diffusion coefficients for the purpose of normalizing other quantities.

4. Discussion

[47] The empirical correlation for D_{eff} developed by OH2008 is among the first meta-analyses of hyporheic exchange (see also *Packman and Salehin* [2003]), and as such represents an important breakthrough in the generalization of single flume experiments into relationships that might be useful for predicting hyporheic exchange across a wide range of laboratory and field conditions. This study builds on the work presented by OH2008, by correcting several errors in the formulas used to estimate effective diffusivity from recirculating and flow-through flume experiments. These errors—which in some cases appeared in the literature several decades before the publication of OH2008—originated when expressions derived for the conduction (with or without convection) of heat from semi-infinite solid bodies were appropriated for hyporheic exchange without making the necessary adjustments for sediment bed porosity.

[48] The 93 values of D_{eff} included in OH2008's meta-analysis were corrected where necessary, and then two empirical correlations were generated by MLR, one based on

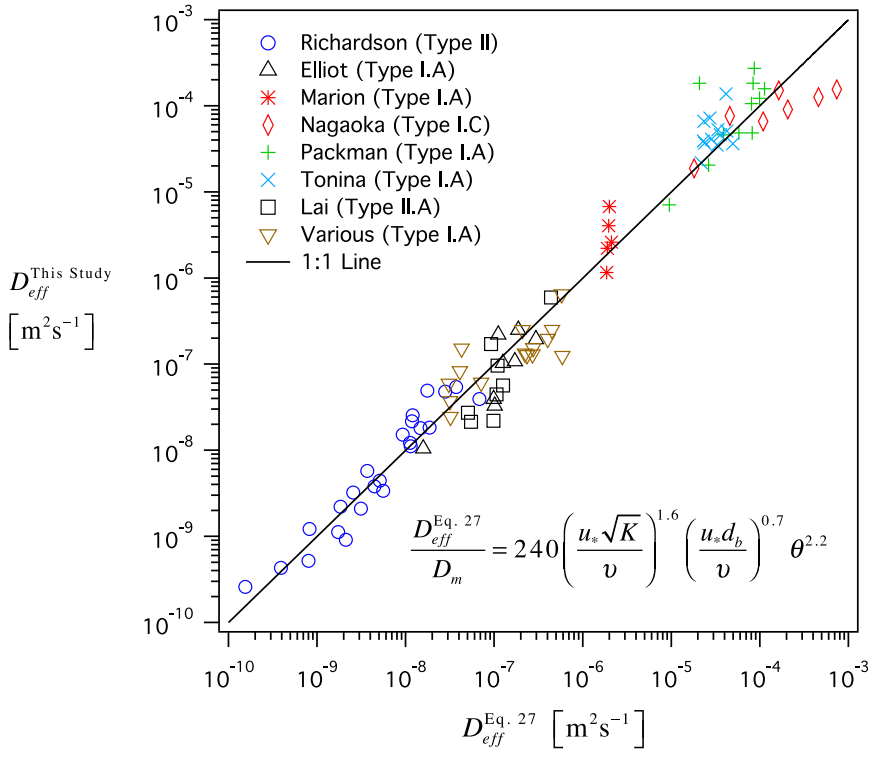

Figure 3. Comparison of measured effective diffusivities with those obtained from equation (27).

the values of primary variables (equation (24)) and another based on the values of nondimensional groupings of the primary variables (equation (27)). Both correlations account for most of the variance in $\log D_{\text{eff}}$ (98% versus 97%), but the latter is dimensionally homogeneous and constructed from dimensionless groups that can yield insights into physical processes that drive hyporheic exchange. The two most important differences between our nondimensional correlation (equation (27)) and the correlation published by OH2008 (equation (1)) are: (1) our correlation does not include the roughness length-scale k_s; and (2) our correlation does include the depth of the sediment bed d_b. The significance of these results is discussed next.

[49] On the face of it, the exclusion of k_s from our correlation is surprising, given $\log D_{\text{eff}}^{\text{This Study}}$ and $\log k_s$ are strongly correlated ($R = 0.89$), and the fact that bed forms and bed roughness are well known to influence hyporheic exchange [*O'Connor and Harvey*, 2007]. But the results are undeniable: in both MLR studies (one with primary variables, and one with nondimensional groupings of primary variables), none of the ten top-ranked models include the roughness length-scale k_s. The reason is that k_s is strongly correlated with several other independent variables, and thus has an inflated VIF (see MLR methods). Because OH2008 did not conduct a formal MLR (they carried out pair-wise correlations between D_{eff} and a set of independent variables), the multicollinearity associated with k_s was not detected in their study. In any case, it is clear from Figures 2 and 3 that k_s is not needed to explain a large percentage of the variance in $\log D_{\text{eff}}/D_m$. Our correlations explain $\geq$ 97% ($R^2 \geq 0.97$) of the variance in $\log D_{\text{eff}}^{\text{This Study}}/D_m$, while OH2008's correlation explained 95% ($R^2 = 0.95$) of the variance in $\log D_{\text{eff}}^{\text{OH2008}}/D'_m$. Furthermore, because the variable D'_m appears on both the right- and left-hand sides of OH2008's correlation, and to roughly the same power ($D_m'^{-1} \sim D_m'^{-6/5}$, see equation (1)), it is likely the R^2 value reported by OH2008 is inflated.

[50] Given the relatively high R^2 values associated with our correlations, it is reasonable to ask: how do they account for the well-documented importance of bed forms and bed roughness on hyporheic exchange? The answer is by inclusion of the shear velocity. The shear velocity reflects the combined influence of flow velocity U and bed friction—for example, as expressed quantitatively by the Darcy-Weisbach friction factor $f_D = 8u_*^2/U^2$—on momentum transport at the sediment-water interface. Thus, our correlation can be expressed explicitly in terms of the friction factor: $D_{\text{eff}} \sim (u_*\sqrt{K})^{1.6}\theta^{2.2} \sim [U\sqrt{f_D K}]^{1.6}\theta^{2.2}$. Because the friction factor depends on bed roughness and the presence of bed forms [*Sturm*, 2001] our correlation for D_{eff} necessarily does as well. Based on experiments conducted in a flow-through (Type II) flume, *Richardson and Parr* [1988] report that effective diffusivity scales with $u_*\sqrt{K}$, although to a power of 2 instead of 1.6: $D_{\text{eff}} \sim [u_*\sqrt{K}]^2 \sim U^2 f_D K$. Because the Darcy-Weisbach friction factor is also a good predictor for reach-scale hyporheic exchange in streams [e.g., *Harvey et al.*, 2003; *Zarnetske et al.*, 2007], it appears f_D parameterizes the effects of bed roughness and bed forms in both laboratory and field measurements of hyporheic exchange.

[51] The other major result to come out of our analysis is the dependence of effective diffusivity measured in laboratory flumes on sediment bed depth d_b. There are several possible explanations for this result. First, laboratory investigations of hyporheic exchange involve establishing a disequilibrium between the concentration of a tracer in the water column and in the sediment bed, and then monitoring the rate at which a new equilibrium is achieved. As the system approaches a new equilibrium, however, the rate of mass exchange across the sediment-water interface is necessarily influenced by the finite size of the sediment bed. Because effective diffusivities are typically calculated using initial rates of change (e.g., initial values of the slopes S, S_ℓ, and S_{m_w}, see Table 1), this seems an unlikely explanation for the dependence of D_{eff} on d_b. Second, pressure variations at the sediment-water interface, induced by periodic bed forms, create an advective flow field within the sediment bed that depends explicitly on sediment bed depth [*Elliot and Brooks*, 1997a; *Packman et al.*, 2000a]. However, this explanation is inconsistent with the fact that our correlations are derived from a collection of different hyporheic exchange studies, some with bed forms (49 out of 93 or 53%) and some without bed forms (44 out of 93 or 47%) (Table 2). Third, numerical simulations of hyporheic exchange indicate long-period pressure fluctuations at the sediment-water interface, caused by coherent turbulence in the water column, can drive flow deep into the sediment bed (up to 0.5 m) [*Boano et al.*, 2011; *Boano et al.*, 2010]. Boano et al.'s numerical result is consistent with several experimental studies of hyporheic exchange in recirculating flumes which document: (1) the existence of well-defined advective flow paths in sediment beds, in the absence of any bed forms that could generate periodic pressure variation at the sediment-water interface [*Packman et al.*, 2004], and (2) the increasing predominance of low-frequency fluctuations in pore fluid velocity with increasing depth below the sediment-water interface, also in the absence of any bed forms that could generate periodic pressure variation at the sediment-water interface [*Nagaoka and Ohgaki*, 1990]. When viewed through the prism of these numerical and experimental results, the inclusion of d_b in our correlations may reflect constraints the sediment bed's vertical dimension imposes on coherent turbulence-driven hyporheic exchange. *Boano et al.'s* [2011] numerical simulations assume the amplitude of coherent motion is equal to 3 to 5 times the depth of the water column, when in fact very large coherent motions, so-called superstructures, can extend over much larger distances [*Hutchins and Marusic*, 2007; *Kim and Adrian*, 1999; *Smits et al.*, 2011], potentially driving hyporheic exchange even deeper below the sediment-water interface. Collectively, these results suggest current approaches for measuring hyporheic exchange in the laboratory may need to be reconceived, to provide a better understanding of the linkage between large-amplitude turbulence in the water column and hyporheic exchange between the stream and streambed.

Appendix A: Raw Data Used for MLR Analyses

[52] Appendix A includes the raw data used for conducting the MLR analysis using either primary variables (Table A1) or nondimensional groupings of primary variables (Table A2).

Table A1. Values of Independent Variables Used in the MLR Described in Section 3.3.1[a]

Candidate Independent Variables								
D_m (m^2 s^{-1})	U (m s^{-1})	u_* (m s^{-1})	k_s(m)	K (m^2)	υ (m^2 s^{-1})	H (m)	d_b (m)	θ(−)
4.75E-10	3.66E-02	3.30E-03	9.48E-03	7.14E-09	1.53E-06	1.30E-02	2.54E-02	0.38
4.75E-10	7.62E-02	5.52E-03	3.14E-03	7.91E-10	9.78E-07	6.35E-03	2.54E-02	0.4
4.75E-10	7.92E-02	7.52E-03	3.14E-03	7.91E-10	9.77E-07	6.35E-03	2.54E-02	0.4
4.75E-10	3.66E-02	2.71E-03	3.14E-03	7.91E-10	1.06E-06	1.30E-02	2.54E-02	0.4
4.75E-10	1.52E-01	1.08E-02	3.14E-03	7.91E-10	1.07E-06	1.30E-02	2.54E-02	0.4
4.75E-10	2.26E-01	1.29E-02	1.54E-03	1.58E-10	1.09E-06	1.35E-02	2.54E-02	0.38
4.75E-10	1.55E-01	9.36E-03	1.54E-03	1.58E-10	1.05E-06	1.27E-02	2.54E-02	0.38
4.75E-10	1.52E-01	1.12E-02	1.54E-03	1.58E-10	1.16E-06	1.24E-02	2.54E-02	0.38
4.75E-10	7.92E-02	5.24E-03	1.54E-03	1.58E-10	1.01E-06	6.60E-03	2.54E-02	0.38
4.75E-10	7.62E-02	8.08E-03	1.54E-03	1.58E-10	1.12E-06	6.60E-03	2.54E-02	0.38
4.75E-10	3.66E-02	2.68E-03	1.54E-03	1.58E-10	1.09E-06	1.27E-02	2.54E-02	0.38
4.75E-10	1.52E-01	8.85E-03	1.54E-03	1.58E-10	1.09E-06	1.88E-02	2.54E-02	0.38
4.75E-10	7.01E-02	4.43E-03	1.54E-03	1.58E-10	1.09E-06	1.88E-02	2.54E-02	0.38
4.75E-10	7.62E-02	6.02E-03	1.54E-03	1.58E-10	1.26E-06	1.93E-02	2.54E-02	0.38
4.75E-10	7.92E-02	5.24E-03	8.88E-04	5.43E-11	9.69E-07	6.60E-03	2.54E-02	0.37
4.75E-10	7.62E-02	7.62E-03	8.88E-04	5.43E-11	9.49E-07	6.60E-03	2.54E-02	0.37
4.75E-10	1.55E-01	8.69E-03	8.88E-04	5.43E-11	1.04E-06	1.27E-02	2.54E-02	0.37
4.75E-10	1.52E-01	1.16E-02	8.88E-04	5.43E-11	1.01E-06	1.24E-02	2.54E-02	0.37
4.75E-10	3.66E-02	2.65E-03	8.88E-04	5.43E-11	1.04E-06	1.30E-02	2.54E-02	0.37
4.75E-10	2.29E-01	1.17E-02	8.88E-04	5.43E-11	1.02E-06	1.30E-02	2.54E-02	0.37
4.75E-10	1.52E-01	1.04E-02	3.30E-04	1.70E-11	1.36E-06	1.27E-02	2.54E-02	0.36
4.75E-10	1.52E-01	N/A	3.30E-04	1.70E-11	1.03E-06	1.27E-02	2.54E-02	0.36
4.75E-10	7.62E-02	7.03E-03	3.30E-04	1.70E-11	1.34E-06	6.60E-03	2.54E-02	0.36
4.75E-10	7.32E-02	1.00E-02	3.30E-04	1.70E-11	1.36E-06	6.86E-03	2.54E-02	0.36
4.75E-10	3.66E-02	3.61E-03	3.30E-04	1.70E-11	1.44E-06	1.30E-02	2.54E-02	0.36
4.1E-10	1.32E-01	1.59E-02	9.46E-03	1.12E-10	1.00E-06	6.45E-02	1.30E-01	0.33
4.1E-10	1.32E-01	2.44E-02	2.89E-02	1.12E-10	1.00E-06	6.45E-02	1.35E-01	0.33
4.1E-10	8.70E-02	1.54E-02	1.54E-02	1.12E-10	1.00E-06	3.10E-02	1.26E-01	0.33
4.1E-10	1.32E-01	1.95E-02	1.54E-02	1.12E-10	1.00E-06	6.48E-02	1.25E-01	0.33
4.1E-10	8.60E-02	1.29E-02	1.54E-02	1.12E-10	1.00E-06	6.48E-02	2.20E-01	0.33
4.1E-10	8.70E-02	1.43E-02	2.89E-02	1.12E-10	1.00E-06	6.48E-02	2.20E-01	0.33
4.1E-10	1.07E-01	1.71E-02	1.97E-02	1.12E-10	1.00E-06	6.48E-02	2.20E-01	0.33
4.1E-10	8.70E-02	1.40E-02	1.29E-02	8.05E-12	1.00E-06	6.45E-02	2.25E-01	0.30
8.7E-10	1.52E-01	1.58E-02	1.21E-02	1.53E-10	1.00E-06	1.27E-01	1.19E-01	0.33
8.7E-10	1.44E-01	1.55E-02	1.18E-02	1.53E-10	1.00E-06	9.00E-02	1.00E-01	0.33
8.7E-10	1.26E-01	1.52E-02	1.50E-02	1.53E-10	1.00E-06	7.90E-02	9.70E-02	0.33
1.5E-09	2.50E-01	1.72E-02	3.38E-03	5.04E-10	1.30E-06	1.09E-01	4.00E-01	0.38
1.5E-09	2.40E-01	1.73E-02	5.40E-03	5.04E-10	1.30E-06	1.10E-01	4.00E-01	0.38
1.5E-09	2.80E-01	1.82E-02	8.49E-03	5.04E-10	1.30E-06	1.18E-01	4.00E-01	0.38
1.5E-09	2.20E-01	1.76E-02	2.36E-02	5.04E-10	1.30E-06	1.23E-01	4.00E-01	0.38
1.5E-09	2.20E-01	1.77E-02	1.80E-02	5.04E-10	1.30E-06	1.21E-01	4.00E-01	0.38
1.5E-09	2.33E-01	1.71E-02	1.66E-02	1.83E-10	1.00E-06	8.70E-02	9.90E-02	0.38
1.5E-09	2.37E-01	1.53E-02	1.72E-02	1.83E-10	1.00E-06	1.18E-01	9.90E-02	0.38
1.5E-09	2.37E-01	1.53E-02	1.72E-02	6.80E-11	1.00E-06	1.18E-01	9.90E-02	0.29
1.5E-09	2.36E-01	1.70E-02	1.59E-02	1.83E-10	1.00E-06	8.60E-02	1.03E-01	0.38
1.5E-09	2.36E-01	1.70E-02	1.59E-02	6.80E-11	1.00E-06	8.60E-02	1.03E-01	0.29
1.5E-09	1.54E-01	6.60E-03	1.32E-02	1.82E-10	1.00E-06	1.09E-01	1.05E-01	0.36
1.5E-09	1.64E-01	1.46E-02	1.58E-02	1.82E-10	1.00E-06	1.04E-01	9.86E-02	0.36
4.75E-10	2.82E-01	5.11E-02	1.16E-01	5.10E-09	1.00E-06	6.50E-02	1.80E-01	0.34
4.75E-10	3.84E-01	5.49E-02	1.16E-01	5.10E-09	1.00E-06	7.50E-02	1.80E-01	0.34
4.75E-10	3.69E-01	4.29E-02	1.16E-01	5.10E-09	1.00E-06	1.04E-01	1.80E-01	0.34
4.75E-10	3.08E-01	4.75E-02	9.40E-02	5.10E-09	1.00E-06	5.60E-02	1.80E-01	0.34
4.75E-10	4.13E-01	5.07E-02	9.40E-02	5.10E-09	1.00E-06	6.40E-02	1.80E-01	0.34
4.75E-10	4.21E-01	3.92E-02	9.40E-02	5.10E-09	1.00E-06	8.70E-02	1.80E-01	0.34
4.75E-10	3.65E-01	4.21E-02	7.92E-02	5.10E-09	1.00E-06	4.40E-02	1.80E-01	0.34
4.75E-10	4.60E-01	4.62E-02	7.92E-02	5.10E-09	1.00E-06	5.30E-02	1.80E-01	0.34
4.75E-10	4.25E-01	3.90E-02	7.92E-02	5.10E-09	1.00E-06	8.60E-02	1.80E-01	0.34
4.75E-10	3.67E-01	3.96E-02	6.40E-02	5.10E-09	1.00E-06	3.90E-02	1.80E-01	0.34
4.75E-10	4.52E-01	4.57E-02	6.40E-02	5.10E-09	1.00E-06	5.20E-02	1.80E-01	0.34
4.75E-10	4.42E-01	3.81E-02	6.40E-02	5.10E-09	1.00E-06	8.20E-02	1.80E-01	0.34
1.5E-09	4.28E-01	4.30E-02	2.45E-01	2.31E-07	1.00E-06	6.75E-02	2.36E-01	0.24
1.5E-09	2.80E-01	4.07E-02	2.45E-01	2.31E-07	1.00E-06	6.75E-02	2.36E-01	0.24
1.5E-09	2.11E-01	2.70E-02	2.45E-01	2.31E-07	1.00E-06	6.75E-02	2.36E-01	0.24
1.5E-09	1.67E-01	2.18E-02	2.45E-01	2.31E-07	1.00E-06	6.75E-02	2.36E-01	0.24
1.5E-09	1.17E-01	1.53E-02	2.45E-01	2.31E-07	1.00E-06	7.00E-02	2.36E-01	0.24
1.5E-09	8.90E-02	1.15E-02	2.45E-01	2.31E-07	1.00E-06	6.75E-02	2.36E-01	0.24
1.5E-09	3.02E-01	2.91E-02	1.14E-01	5.02E-08	1.00E-06	3.20E-02	1.15E-01	0.24
1.5E-09	2.03E-01	1.65E-02	1.14E-01	5.02E-08	1.00E-06	3.20E-02	1.15E-01	0.24
1.5E-09	1.12E-01	1.09E-02	1.14E-01	5.02E-08	1.00E-06	3.20E-02	1.15E-01	0.24

Table A1. (continued)

Candidate Independent Variables								
D_m (m^2 s^{-1})	U (m s^{-1})	u_* (m s^{-1})	k_s(m)	K (m^2)	υ (m^2 s^{-1})	H (m)	d_b (m)	$\theta(-)$
1.5E-09	1.30E-01	4.82E-03	1.31E-02	1.82E-10	1.00E-06	7.90E-02	9.24E-02	0.36
1.5E-09	1.44E-01	4.56E-03	1.14E-02	1.82E-10	1.00E-06	7.07E-02	1.04E-01	0.36
1.5E-09	1.41E-01	4.64E-03	9.05E-03	1.82E-10	1.00E-06	7.30E-02	1.02E-01	0.36
1.5E-09	1.20E-01	5.05E-03	9.57E-03	1.82E-10	1.00E-06	8.65E-02	1.14E-01	0.36
1.5E-09	1.57E-01	5.15E-03	9.09E-03	1.82E-10	1.00E-06	9.00E-02	1.13E-01	0.36
1.5E-09	1.54E-01	5.97E-03	2.07E-02	1.86E-09	1.00E-06	9.70E-03	1.50E-01	0.38
1.5E-09	7.41E-02	2.36E-03	2.07E-02	1.86E-09	1.00E-06	2.02E-02	1.50E-01	0.38
1.5E-09	1.01E-01	3.42E-03	2.07E-02	1.86E-09	1.00E-06	1.99E-02	1.50E-01	0.38
1.5E-09	9.88E-02	3.38E-03	1.25E-02	1.29E-09	1.00E-06	5.10E-03	1.50E-01	0.38
1.5E-09	9.88E-02	3.59E-03	1.25E-02	1.29E-09	1.00E-06	1.01E-02	1.50E-01	0.38
1.5E-09	9.98E-02	3.47E-03	1.25E-02	1.29E-09	1.00E-06	1.50E-02	1.50E-01	0.38
1.5E-09	9.98E-02	4.71E-03	7.01E-03	6.10E-10	1.00E-06	5.00E-03	1.50E-01	0.37
1.5E-09	1.01E-01	4.68E-03	3.54E-03	2.31E-10	1.00E-06	4.90E-03	1.50E-01	0.36
1.5E-09	3.61E-01	3.19E-02	5.26E-02	1.53E-08	1.00E-06	1.14E-01	1.90E-01	0.38
1.5E-09	2.74E-01	2.75E-02	5.26E-02	1.53E-08	1.00E-06	1.13E-01	1.90E-01	0.38
1.5E-09	1.79E-01	1.98E-02	5.26E-02	1.53E-08	1.00E-06	1.14E-01	1.90E-01	0.38
1.5E-09	9.10E-02	1.06E-02	5.26E-02	1.53E-08	1.00E-06	1.14E-01	1.90E-01	0.38
1.5E-09	1.79E-01	3.01E-02	5.26E-02	1.53E-08	1.00E-06	2.01E-01	1.90E-01	0.38
1.5E-09	9.20E-02	1.67E-02	5.26E-02	1.53E-08	1.00E-06	2.02E-01	1.90E-01	0.38
1.5E-09	1.77E-01	2.79E-02	6.48E-02	1.53E-08	1.00E-06	2.04E-01	1.90E-01	0.38
1.5E-09	9.00E-02	2.76E-02	6.48E-02	1.53E-08	1.00E-06	2.05E-01	1.90E-01	0.38
1.5E-09	2.68E-01	2.83E-02	4.62E-02	1.53E-08	1.00E-06	2.04E-01	1.90E-01	0.38
1.5E-09	1.77E-01	1.50E-02	4.62E-02	1.53E-08	1.00E-06	2.03E-01	1.90E-01	0.38
1.5E-09	9.10E-02	2.37E-02	4.62E-02	1.53E-08	1.00E-06	2.04E-01	1.90E-01	0.38

[a]Compiled data kindly provided by Dr. Ben O'Connor. Rows in this table correspond to the 93 flume experiments summarized in Table 2.

Table A2. Values of Dependent and Independent Nondimensional Groups Used in the MLR Described in Section 3.3.2[a]

Dependent Variable	Candidate Independent Nondimensional Variables						
$\frac{D_{\text{eff}}^{\text{This Study}}}{D_m}$	$Re = \frac{UH}{\upsilon}$	$Re_k = \frac{u_* k_s}{\upsilon}$	$Re_* = \frac{u_* H}{\upsilon}$	$Pe_* = \frac{u_* \sqrt{K}}{\upsilon}$	$Sc = \frac{\upsilon}{D_m}$	θ	$\frac{u_* d_b}{\upsilon}$
4.56E+01	3.10E+02	2.04E+01	2.79E+01	1.82E-01	3.22E+03	3.80E-01	5.48E+01
3.85E+01	4.95E+02	1.77E+01	3.59E+01	1.59E-01	2.06E+03	4.00E-01	1.43E+02
1.14E+02	5.15E+02	2.41E+01	4.89E+01	2.16E-01	2.06E+03	4.00E-01	1.95E+02
4.42E+00	4.45E+02	7.99E+00	3.30E+01	7.16E-02	2.24E+03	4.00E-01	6.47E+01
8.27E+01	1.85E+03	3.17E+01	1.31E+02	2.84E-01	2.25E+03	4.00E-01	2.56E+02
1.01E+02	2.80E+03	1.82E+01	1.59E+02	1.49E-01	2.29E+03	3.80E-01	3.01E+02
3.82E+01	1.88E+03	1.37E+01	1.13E+02	1.12E-01	2.22E+03	3.80E-01	2.26E+02
1.04E+02	1.64E+03	1.48E+01	1.20E+02	1.21E-01	2.44E+03	3.80E-01	2.45E+02
8.01E+00	5.20E+02	8.00E+00	3.44E+01	6.55E-02	2.12E+03	3.80E-01	1.32E+02
3.21E+01	4.50E+02	1.11E+01	4.77E+01	9.08E-02	2.35E+03	3.80E-01	1.84E+02
2.57E+00	4.25E+02	3.77E+00	3.12E+01	3.08E-02	2.30E+03	3.80E-01	6.23E+01
5.37E+01	2.63E+03	1.25E+01	1.52E+02	1.02E-01	2.30E+03	3.80E-01	2.06E+02
6.79E+00	1.21E+03	6.25E+00	7.65E+01	5.12E-02	2.29E+03	3.80E-01	1.03E+02
1.21E+01	1.17E+03	7.36E+00	9.25E+01	6.02E-02	2.65E+03	3.80E-01	1.22E+02
1.92E+00	5.40E+02	4.80E+00	3.57E+01	3.98E-02	2.04E+03	3.70E-01	1.37E+02
9.36E+00	5.30E+02	7.13E+00	5.30E+01	5.91E-02	2.00E+03	3.70E-01	2.04E+02
7.12E+00	1.90E+03	7.41E+00	1.06E+02	6.14E-02	2.19E+03	3.70E-01	2.12E+02
2.57E+01	1.87E+03	1.01E+01	1.42E+02	8.39E-02	2.14E+03	3.70E-01	2.89E+02
9.05E-01	4.55E+02	2.26E+00	3.30E+01	1.87E-02	2.19E+03	3.70E-01	6.46E+01
2.33E+01	2.90E+03	1.02E+01	1.49E+02	8.45E-02	2.15E+03	3.70E-01	2.91E+02
4.65E+00	1.42E+03	2.51E+00	9.66E+01	3.14E-02	2.87E+03	3.60E-01	1.93E+02
5.38E+00	1.88E+03	N/A	N/A	N/A	2.17E+03	3.60E-01	N/A
1.10E+00	3.75E+02	1.73E+00	3.46E+01	2.16E-02	2.83E+03	3.60E-01	1.33E+02
2.36E+00	3.70E+02	2.44E+00	5.07E+01	3.05E-02	2.85E+03	3.60E-01	1.88E+02
5.46E-01	3.30E+02	8.30E-01	3.26E+01	1.04E-02	3.02E+03	3.60E-01	6.39E+01
5.36E+02	8.51E+03	1.51E+02	1.03E+03	1.68E-01	2.44E+03	3.25E-01	2.07E+03
4.76E+02	8.51E+03	7.05E+02	1.57E+03	2.58E-01	2.44E+03	3.25E-01	3.29E+03
8.03E+01	2.70E+03	2.37E+02	4.77E+02	1.63E-01	2.44E+03	3.25E-01	1.94E+03
2.64E+02	8.55E+03	3.00E+02	1.27E+03	2.07E-01	2.44E+03	3.25E-01	2.44E+03
9.59E+01	5.57E+03	1.98E+02	8.33E+02	1.36E-01	2.44E+03	3.25E-01	2.83E+03
2.50E+02	5.64E+03	4.13E+02	9.24E+02	1.51E-01	2.44E+03	3.25E-01	3.14E+03
6.10E+02	6.93E+03	3.36E+02	1.11E+03	1.81E-01	2.44E+03	3.25E-01	3.76E+03

Table A2. (continued)

Dependent Variable	Candidate Independent Nondimensional Variables						
$\frac{D_{\text{eff}}^{\text{This Study}}}{D_m}$	$Re = \frac{UH}{\upsilon}$	$Re_k = \frac{u_* k_s}{\upsilon}$	$Re_* = \frac{u_* H}{\upsilon}$	$Pe_* = \frac{u_* \sqrt{K}}{\upsilon}$	$Sc = \frac{\upsilon}{D_m}$	θ	$\frac{u_* d_b}{\upsilon}$
2.56E+01	5.61E+03	1.80E+02	9.03E+02	3.97E-02	2.44E+03	2.95E-01	3.15E+03
1.77E+02	1.93E+04	1.91E+02	2.00E+03	1.95E-01	1.15E+03	3.25E-01	1.88E+03
1.47E+02	1.30E+04	1.84E+02	1.40E+03	1.92E-01	1.15E+03	3.25E-01	1.55E+03
1.53E+02	9.95E+03	2.29E+02	1.20E+03	1.89E-01	1.15E+03	3.25E-01	1.48E+03
7.76E+02	2.10E+04	4.46E+01	1.44E+03	2.97E-01	8.67E+02	3.80E-01	5.29E+03
1.48E+03	2.02E+04	7.18E+01	1.46E+03	2.98E-01	8.67E+02	3.80E-01	5.32E+03
1.74E+03	2.53E+04	1.19E+02	1.64E+03	3.14E-01	8.67E+02	3.80E-01	5.60E+03
2.71E+03	2.08E+04	3.19E+02	1.67E+03	3.04E-01	8.67E+02	3.80E-01	5.41E+03
4.52E+03	2.05E+04	2.46E+02	1.65E+03	3.06E-01	8.67E+02	3.80E-01	5.46E+03
4.33E+02	2.03E+04	2.83E+02	1.49E+03	2.32E-01	6.67E+02	3.80E-01	1.69E+03
1.67E+02	2.80E+04	2.63E+02	1.81E+03	2.07E-01	6.67E+02	3.80E-01	1.51E+03
1.66E+02	2.80E+04	2.63E+02	1.81E+03	1.26E-01	6.67E+02	2.90E-01	1.51E+03
8.34E+01	2.03E+04	2.70E+02	1.46E+03	2.30E-01	6.67E+02	3.80E-01	1.75E+03
8.64E+01	2.03E+04	2.70E+02	1.46E+03	1.40E-01	6.67E+02	2.90E-01	1.75E+03
4.08E+01	1.67E+04	8.73E+01	7.17E+02	8.90E-02	6.67E+02	3.60E-01	6.96E+02
1.31E+02	1.71E+04	2.31E+02	1.52E+03	1.97E-01	6.67E+02	3.60E-01	1.44E+03
1.07E+05	1.83E+04	5.92E+03	3.32E+03	3.65E+00	2.11E+03	3.40E-01	9.20E+03
7.66E+04	2.88E+04	6.36E+03	4.12E+03	3.92E+00	2.11E+03	3.40E-01	9.89E+03
8.62E+04	3.84E+04	4.96E+03	4.46E+03	3.06E+00	2.11E+03	3.40E-01	7.71E+03
9.71E+04	1.72E+04	4.46E+03	2.66E+03	3.39E+00	2.11E+03	3.40E-01	8.54E+03
2.91E+05	2.64E+04	4.77E+03	3.25E+03	3.62E+00	2.11E+03	3.40E-01	9.13E+03
1.39E+05	3.66E+04	3.68E+03	3.41E+03	2.80E+00	2.11E+03	3.40E-01	7.06E+03
1.52E+05	1.61E+04	3.33E+03	1.85E+03	3.00E+00	2.11E+03	3.40E-01	7.57E+03
1.12E+05	2.44E+04	3.66E+03	2.45E+03	3.30E+00	2.11E+03	3.40E-01	8.31E+03
8.22E+04	3.66E+04	3.09E+03	3.35E+03	2.78E+00	2.11E+03	3.40E-01	7.01E+03
7.76E+04	1.43E+04	2.53E+03	1.54E+03	2.83E+00	2.11E+03	3.40E-01	7.13E+03
7.38E+04	2.35E+04	2.93E+03	2.38E+03	3.26E+00	2.11E+03	3.40E-01	8.23E+03
4.59E+04	3.62E+04	2.44E+03	3.12E+03	2.72E+00	2.11E+03	3.40E-01	6.85E+03
4.30E+05	2.89E+04	1.05E+04	2.90E+03	2.07E+01	6.67E+02	2.42E-01	1.01E+04
2.89E+05	1.89E+04	9.96E+03	2.75E+03	1.96E+01	6.67E+02	2.42E-01	9.61E+03
1.03E+05	1.42E+04	6.61E+03	1.82E+03	1.30E+01	6.67E+02	2.42E-01	6.37E+03
8.38E+04	1.13E+04	5.34E+03	1.47E+03	1.05E+01	6.67E+02	2.42E-01	5.14E+03
6.06E+04	8.19E+03	3.75E+03	1.07E+03	7.36E+00	6.67E+02	2.42E-01	3.61E+03
4.39E+04	6.01E+03	2.82E+03	7.76E+02	5.53E+00	6.67E+02	2.42E-01	2.71E+03
1.00E+05	9.66E+03	3.32E+03	9.31E+02	6.52E+00	6.67E+02	2.42E-01	3.35E+03
5.08E+04	6.50E+03	1.88E+03	5.28E+02	3.70E+00	6.67E+02	2.42E-01	1.90E+03
1.25E+04	3.58E+03	1.24E+03	3.49E+02	2.44E+00	6.67E+02	2.42E-01	1.25E+03
1.62E+01	1.03E+04	6.30E+01	3.81E+02	6.50E-02	6.67E+02	3.60E-01	4.46E+02
3.96E+01	1.02E+04	5.21E+01	3.22E+02	6.15E-02	6.67E+02	3.60E-01	4.73E+02
2.48E+01	1.03E+04	4.19E+01	3.38E+02	6.25E-02	6.67E+02	3.60E-01	4.75E+02
5.53E+01	1.03E+04	4.83E+01	4.36E+02	6.81E-02	6.67E+02	3.60E-01	5.74E+02
1.01E+02	1.41E+04	4.68E+01	4.63E+02	6.94E-02	6.67E+02	3.60E-01	5.83E+02
3.96E+02	1.49E+03	1.23E+02	5.79E+01	2.57E-01	6.67E+02	3.80E-01	8.95E+02
1.43E+01	1.50E+03	4.87E+01	4.76E+01	1.02E-01	6.67E+02	3.80E-01	3.53E+02
3.77E+01	2.01E+03	7.08E+01	6.81E+01	1.48E-01	6.67E+02	3.80E-01	5.13E+02
1.14E+02	5.04E+02	4.22E+01	1.72E+01	1.21E-01	6.67E+02	3.80E-01	5.07E+02
2.97E+01	9.98E+02	4.48E+01	3.62E+01	1.29E-01	6.67E+02	3.80E-01	5.38E+02
1.46E+01	1.50E+03	4.34E+01	5.21E+01	1.25E-01	6.67E+02	3.80E-01	5.21E+02
6.41E+01	4.99E+02	3.30E+01	2.35E+01	1.16E-01	6.67E+02	3.70E-01	7.06E+02
1.82E+01	4.95E+02	1.66E+01	2.29E+01	7.12E-02	6.67E+02	3.60E-01	7.02E+02
1.06E+05	4.12E+04	1.68E+03	3.64E+03	3.94E+00	6.67E+02	3.80E-01	6.06E+03
7.06E+04	3.10E+04	1.45E+03	3.10E+03	3.39E+00	6.67E+02	3.80E-01	5.22E+03
3.07E+04	2.04E+04	1.04E+03	2.26E+03	2.45E+00	6.67E+02	3.80E-01	3.76E+03
4.72E+03	1.04E+04	5.57E+02	1.21E+03	1.31E+00	6.67E+02	3.80E-01	2.01E+03
8.15E+04	3.60E+04	1.59E+03	6.05E+03	3.72E+00	6.67E+02	3.80E-01	5.72E+03
1.37E+04	1.86E+04	8.77E+02	3.36E+03	2.06E+00	6.67E+02	3.80E-01	3.16E+03
1.22E+05	3.61E+04	1.81E+03	5.70E+03	3.45E+00	6.67E+02	3.80E-01	5.31E+03
3.23E+04	1.85E+04	1.79E+03	5.67E+03	3.42E+00	6.67E+02	3.80E-01	5.25E+03
1.82E+05	5.47E+04	1.31E+03	5.77E+03	3.50E+00	6.67E+02	3.80E-01	5.38E+03
1.22E+05	3.59E+04	6.93E+02	3.05E+03	1.85E+00	6.67E+02	3.80E-01	2.85E+03
3.23E+04	1.86E+04	1.09E+03	4.83E+03	2.93E+00	6.67E+02	3.80E-01	4.50E+03

[a]Raw data used to calculate values of the nondimensional groups were kindly provided by Dr. Ben O'Connor, and are listed in Table A1. Rows in this table correspond to the 93 flume experiments summarized in Table 2.

[53] **Acknowledgments.** Financial support provided by a 2011 UCI Henry Samueli School of Engineering Research Ignition Fund and a National Science Foundation Award 0724806 (to SBG); awards from the Australian Research Council and the University of Melbourne School of Engineering Iconic Research Project (to IM), and Australian Research Council Linkage Project (LP100200170) (to MS). The authors especially thank O'Connor for providing compiled data used in his meta-analysis of hyporheic exchange [*O'Connor and Harvey*, 2008] and Tonina for providing raw data from a set of recirculating flume experiments [*Tonina and Buffington*, 2007]. The manuscript was greatly improved based on feedback from four anonymous reviewers.

References

Akaike, H. (1974), A new look at the statistical model identification, *IEEE Trans. Autom. Control*, *19*(6), 716–723, doi:10.1109/TAC.1974.1100705.

Bencala, K. E., M. N. Gooseff, and B. A. Kimball (2011), Rethinking hyporheic flow and transient storage to advance understanding of stream-catchment connections, *Water Resour. Res.*, *47*, W00H03, doi:10.1029/2010WR010066.

Boano, F., C. Manes, D. Poggi, R. Revelli, and L. Ridolfi (2010), Comment on "pore water flow due to near-bed turbulence and associated solute transfer in a stream or lake sediment bed" by M. Hiashino et al., *Water Resour. Res.*, *46*, W10801, doi:10.1029/2010WR009185.

Boano, F., R. Revelli, and L. Ridolfi (2011), Water and solute exchange through flat streambeds induced by large turbulent eddies, *J. Hydrol.*, *402*, 290–296.

Boulton, A. J. (2007), Hyporheic rehabilitation in rivers: Restoring vertical connectivity, *Freshwater Biol.*, *52*(4), 532–650.

Boulton, A. J., T. Datry, T. Kasahara, M. Mutz, and J. A. Stanford (2010), Ecology and management of the hyporheic zone: Stream-groundwater interactions of running waters and their floodplains, *J. North Am. Benthol. Soc.*, *29*(1), 26–40.

Brunke, M., and T. Gosner (1997), The ecological significance of exchange processes between rivers and groundwater, *Freshwater Biol.*, *73*(1), 1–33.

Buss, S., et al. (2009), The Hyporheic Handbook: A handbook on the groundwater-surface water interface and hyporheic zone for environment managers, Integrated Catchment Science Programme, *Science report SC040070*, Environment Agency, Bristol, U.K.

Dole-Olivier, M. J., P. Marmonier, and J. L. Beffy (1997), Response of invertebrates to lotic disturbance: Is the hyporheic zone a patchy refugium?, *Freshwater Biol.*, *37*(2), 257–276.

Elliot, A. H. (1991), Transfer of solutes into and out of streambeds, PhD thesis, Department of Environmental Engineering Science, California Institute of Technology, Pasadena, Calif.

Elliott, A. H. and N. H. Brooks (1997a), Transfer of nonsorbing solutes to a streambed with bedforms: Theory, *Water Resour. Res.*, *33*(1), 123–136.

Elliott, A. H., and N. H. Brooks (1997b), Transfer of nonsorbing solutes to a streambed with bed forms: Laboratory experiments, *Water Resour. Res.*, *33*(1), 137–151.

Fischer, H. B., E. J. List, R. C. Y. Koh, J. Imberger, N. A. Brooks (1979), *Mixing in Inland and Coast Waters*, Academic, New York.

Frick, W. E., Z. Ge, and R. G. Zepp (2008), Nowcasting and forecasting concentrations of biological contamination at beaches: A feasibility and case study, *Environ. Sci. Technol.*, *42*(13), 4818–4824.

Fries, J. S. (2007), Predicting interfacial diffusion coefficients for fluxes across the sediment-water interface, *ASCE J. Hydraul. Eng.*, *133*(3), 267–272, doi:10.1061/(ASCE)0733-9429(2007)133:3(267).

Gandy, C. J., J. W. N. Smith, and A. P. Jarvis (2007), Attenuation of mining-derived pollutants in the hyporheic zone: A review, *Sci. Total Environ.*, *373*, 435–446.

Ge, Z., and W. E. Frick (2007), Some statistical issues related to multiple linear regression modeling of beach bacteria concentrations, *Environ. Res.*, *103*(3), 358–364.

Grant, S. B., and I. Marusic (2011), Crossing turbulent boundaries: Interfacial flux in environmental flows, *Environ. Sci. Technol.*, *45*, 7107–7113, dx.doi.org/10.1021/es201778s.

Greig, S. M., D. A. Sear, and P. A. Carling (2007), A review of factors influencing the availability of dissolved oxygen to incubating salmonid embryos, *Hydrol. Processes*, *21*(3), 323–334.

Hancock, P. J. (2002), Human impacts on the stream-groundwater exchange zone, *Environ. Manage.*, *29*(6), 763–781.

Harvey, J. W., M. H. Conklin, and R. S. Koelsch (2003), Predicting changes in hydrologic retention in an evolving semi-arid alluvial stream, *Adv. Water Resour.*, *26*, 939–950.

Hester, E. T., and M. N. Gooseff (2010), Moving beyond the banks: Hyporheic restoration is fundamental to restoring ecological services and functions of streams, *Environ. Sci. Technol.*, *44*, 1521–1525.

Higashino, M., J. J. Clark, and H. G. Stefan (2009), Pore water flow due to near-bed turbulence and associated solute transfer in a stream or lake sediment bed, *Water Resour. Res.*, *45*, W12414, doi:10.1029/2008WR007374.

Hinkle, S. R., J. H. Duff, F. J. Triska, A. Laenen, E. G. Gates, K. E. Bencala, D. A. Wentz, and S. R. Silva (2001), Linking hyporheic flow and nitrogen cycling near the Willamette River—A large river in Oregon, USA, *J. Hydrol.*, *244*(3–4), 157–180.

Hutchins, N., and I. Marusic (2007), Evidence of very long meandering features in the logarithmic region of turbulent boundary layers, *J. Fluid Mech.*, *579*, 1–28.

Incropera, F. P., D. P. Dewitt, T. L. Bergman, and A. S. Lavine (2007), *Fundamentals of Heat and Mass Transfer*, John Wiley, Hoboken, NJ.

Iverson, N., and B. B. Jorgensen (1993), Diffusion coefficients of sulfate and methane in marine sediments: Influence of porosity, *Geochim. Cosmochim. Acta*, *57*, 571–578.

Kasahara, T., T. Datry, T. M. Mutz and A. J. Boulton (2009), Treating causes not symptoms: Restoration of surface-groundwater interactions in rivers, *Mar. Freshwater Res.*, *60*(9), 976–981.

Kim, K. C., and R. J. Adrian (1999), Very large-scale motion in the outer layer, *Phys. Fluids*, *11*, 417–422.

Lai, J. L., S. L. Lo, and C. F. Lin (1994), Effects of hydraulic and medium characteristics on solute transfer to surface runoff, *Water Sci. Technol.*, *30*(7), 145–155.

Longnecker, M. T., and R. L. Ott (2004), *A First Course in Statistical Methods*, Thomas Brooks/Cole, Belmont, Calif.

Malard, F., K. Tockner, M.-J. Dole-Olivier, and J. V. Ward (2002), A landscape perspective of surface-subsurface hydrological exchanges in river corridors, *Freshwater Biol.*, *47*(4), 621–640.

Marion, A., M. Bellinello, I. Guymer, and A. Packman (2002), Effect of bed form geometry on the penetration of nonreactive solutes into a streambed, *Water Resour. Res.*, *38*(10), 1209 doi:10.1029/2001WR000264.

Nagaoka, H., and S. Ohgaki (1990), Mass transfer mechanism in a porous riverbed, *Water Res.*, *24*(4), 417–425.

O'Connor, B. L., and J. W. Harvey (2008), Scaling hyporheic exchange and its influence on biogeochemical reactions in aquatic ecosystems, *Water Resour. Res.*, *44*, W12423, doi:10.1029/2008WR007160.

Packman, A. I., and J. S. MacKay (2003), Interplay of stream-subsurface exchange, clay particle deposition, and streambed evolution, *Water Resour. Res.*, *39*(4), 1097, doi:10.1029/2002WR001432.

Packman, A. I., and M. Salehin (2003), Relative roles of stream flow and sedimentary conditions in controlling hyporheic exchange, *Hydrobiologia*, *494*, 291–297.

Packman, A. I., N. H. Brooks, and J. J. Morgan (2000a), A physicochemical model for colloid exchange between a stream and a sand streambed with bed forms, *Water Resour. Res.*, *36*(8), 2351–2361.

Packman, A. I., N. H. Brooks, and J. J. Morgan (2000b), Kaolinite exchange between a stream and streambed: Laboratory experiments and validation of a colloid transport model, *Water Resour. Res.*, *36*(8), 2363–2372.

Packman, A. I., M. Salehin, and M. Zaramella (2004), Hyporheic exchange with gravel beds: Basic hydrodynamic interactions and bedform-induced advective flows, *ASCE J. Hydraul. Eng.*, *130*(7), 647–656.

Parr, A. D., C. Richardson, D. D. Lane, D. Baughman (1987), Pore water uptake by agricultural runoff, *ASCE J. Environ. Eng.*, *113*, 49–63.

Pinay, G., T. C. O'Keefe, R. T. Edwards, and R. J. Naiman (2009), Nitrate removal in the hyporheic zone of a salmon river in Alaska, *River Res. Appl.*, *25*, 367–375.

Rehg, K. J., A. I. Packman, and J. Ren (2005), Effects of suspended sediment characteristics and bed sediment transport on streambed clogging, *Hydrol. Processes*, *19*, 413–427.

Reidenbach, A., M. Limm, M. Hondzo, and M. T. Stacey (2010), Effects of bed roughness on boundary layer mixing and mass flux across the sediment-water interface, *Water Resour. Res.*, *46*, W07530, doi:10.1029/2009WR008248.

Ren, J., and A. I. Packman (2004), Stream-subsurface exchange of zinc in the presence of silica and kaolinite colloids, *Environ. Sci. Technol.*, *38*, 6571–6581.

Richardson, C. P., and A. D. Parr (1988), Modified Fickian model for solute uptake by runoff, *ASCE J. Environ. Eng.*, *114*, 792–809.

Smits, A. J., B. J. McKeon, and I. Marusic (2011), High Reynolds number wall turbulence, *Ann. Rev. Fluid Mech.*, *43*, 353–375.

Stonedahl, S. H., J. W. Harvey, A. Worman, M. Salehin, and A. I. Packman (2010), A multiscale model for integrating hyporheic exchange from

ripples to meanders, *Water Resour. Res.*, *46*, W12539, doi:10.1029/2009WR008865.

Sturm, T. W. (2001), *Open Channel Hydraulics*, McGraw Hill, New York.

Tonina, D., and J. M. Buffington (2007), Hyporheic exchange in gravel bed rivers with pool-riffle morphology: Laboratory experiments and three-dimensional modeling, *Water Resour. Res.*, *43*, W01421, doi:10.1029/2005WR004328.

van Rijn, L. C. (1984), Sediment transport, part III: Bed forms and alluvial roughness, *J. Hydraul. Eng.*, *110*, 1733–1754.

Wood, P. J., A. J. Boulton, S. Little, and R. Stubbington (2010), Is the hyporheic zone a refugium for aquatic macroinvertebrates during severe low flow conditions?, *Fundam. Appl. Limnol.*, *176*(4), 377–390.

Worman, A., A. I. Packman, H. Johansson, and K. Jonsson (2002), Effect of flow-induced exchange in hyporheic zones on longitudinal transport of solutes in streams and rivers, *Water Resour. Res.*, *38*(1), 1001, doi:10.1029/2001WR000769.

Zarnetske, J. P., M. N. Gooseff, T. R. Brosten, J. H. Bradford, J. P. McNamara, and W. B. Bowden (2007), Transient storage as a function of geomorphology, discharge, and permafrost active layer conditions in arctic tundra streams, *Water Resour. Res.*, *43*, W07410, doi:10.1029/2005WR004816.

S. B. Grant, Department of Civil and Environmental Engineering, E4130 Engineering Gateway, University of California, Irvine, Irvine, CA 92697-2175, USA. (sbgrant@uci.edu)

I. Marusic, Department of Mechanical Engineering, Engineering Block E, Melbourne School of Engineering, University of Melbourne, Parkville 3010, Victoria, Australia.

M. J. Stewardson, Department of Infrastructure Engineering, Engineering Block D, Melbourne School of Engineering, University of Melbourne, Parkville 3010, Victoria, Australia.